

## Imaging and Engineering the Nanoscale-domain Structure of a $\text{Sr}_{0.61}\text{Ba}_{0.39}\text{Nb}_2\text{O}_6$ Crystal

Shinji Higuchi<sup>\*,\*\*</sup>, Kazuya Terabe<sup>\*</sup>, Masaru Nakamura<sup>\*</sup>, Shunji Takekawa<sup>\*</sup>,  
Yoshihiko Gotoh<sup>\*\*</sup>, and Kenji Kitamura<sup>\*</sup>

<sup>\*</sup>National Institute for Materials Science, 1-1 Namiki, Tsukuba-shi, Ibaraki 305-0044, Japan  
Fax: 81-298-51-6159, e-mail: TERABE.Kazuya@nims.go.jp

<sup>\*\*</sup>Department of Materials Science and Technology, Tokyo University of Science,  
2641 Yamazaki, Noda-shi, Chiba 278-8510, Japan

We have investigated the ferroelectric domain structure formed in a  $\text{Sr}_{0.61}\text{Ba}_{0.39}\text{Nb}_2\text{O}_6$  (SBN) single crystal by cooling the crystal through the Curie point. The SBN crystal was grown by a newly developed double-crucible Stepanov method. Imaging the etched surface structure using a scanning force microscope in both the topographic mode and the piezoresponse mode revealed that a multidomain structure of nanoscale island-like domains was formed in the SBN crystal. Furthermore, tailored patterns of inverted-domain structure were fabricated using the thin SBN sample which underwent poling treatment, where polarization directions of the domains were locally switched by scanning the samples with a conductive cantilever while applying voltages.

Key words: scanning force microscope, ferroelectric domain, domain engineering, nanoscale fabrication, SBN

### 1. INTRODUCTION

Ferroelectric single crystals have been used as materials for functional devices because they have various properties, such as electrooptic, nonlinear optic and piezoelectric properties and the photorefractive effect; strontium barium niobate ( $\text{Sr}_{0.61}\text{Ba}_{0.39}\text{Nb}_2\text{O}_6$ ; SBN, hereafter) is one of ferroelectric crystals. Several functional devices, such as light modulation and holographic memory devices, have been produced thus far by exploiting the superior properties of SBN crystals. Recently, the development of functional devices utilizing the functions and characteristics obtained by patterning microscale domain structures in ferroelectric crystals such as the SBN and  $\text{LiNbO}_3$  crystals has attracted attention. Thus far, second-harmonic generation (SHG) devices [1] and optical parametric oscillation devices [2] have been fabricated by exploiting quasi phase-matching (QPM) in the construction of a microscale periodically inverted-domain structure [3]. We anticipate the creation of functional devices that exploit the characteristics newly exhibited through the domain structure of ferroelectric crystals artificially structured at the nanoscale level in the future [4,5].

Recently, it has been found that SHG was emitted from an as-grown SBN crystal, in which the periodically inverted-domain structure was not formed artificially [6]. This is possible because a multidomain structure is naturally formed in the SBN crystal upon cooling through the Curie point ( $T_c$ ), and these domains partially satisfy the QPM condition. On the basis of observations made using a transmission electron microscope, the formation of nanoscale  $180^\circ$  domains with the polarization that is parallel to the  $c$ -axis of the SBN crystal has been revealed [7]. However, the domain structure formed in the SBN crystal has not been investigated due to the difficulty in domain visualization using conventional optical microscopy.

We have investigated the imaging and engineering of the domain structure in the SBN crystal using a scanning force microscope (SFM). Imaging the etched SBN surface in both the topographic and piezoresponse [4,8-10] modes of the SFM revealed the nanoscale multidomain structure in the as-grown SBN crystal. Furthermore, inversion of the domains was achieved by applying an appropriate dc bias voltage using the conductive SFM tip [4,8,9,11]. Tailored-patterns of inverted-domain structure were fabricated using the SFM. It was difficult to fabricate the nanoscale domain patterns by conventional electric field poling using lithographically defined electrodes [12].

### 2. EXPERIMENTAL METHOD

A single crystal of SBN was grown by a newly developed double-crucible Stepanov method [13]. The as-grown crystal was annealed at  $1350^\circ\text{C}$  for 24 h and then cooled to room temperature in the furnace. The crystal was cut perpendicular to the  $c$ -axis, and polished using alumina powder and colloidal silica solutions. Then, the crystal was etched in a HF aqueous solution at room temperature for 10 minutes. Imaging of the domain structure on the etched SBN surface was achieved using the SFM in two different modes. First, the etched surface was scanned in the topographic mode. The domain structure could be revealed in the topographic mode due to the different etching behaviors of the positive and negative polarized faces of domains. Second, the conductive SFM tip was used to perform domain imaging in the piezoresponse mode with an applied ac bias voltage of 10-14 V (peak-to-peak) at a frequency of 10 kHz. The piezoresponse mode is expected to be able to directly image the domain structures with nanoscale resolution. The piezoresponse and topographic visualizations of domain structures on the etched surface of the crystal were used as

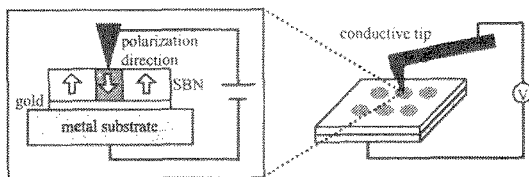


Fig.1 Domain engineering method by using SFM. Polarization directions of domains were locally switched by applying bias voltage using a conductive SFM cantilever.

complementary methods to confirm the suitability of using the SFM approach for the SBN crystal.

The domain engineering of the SBN crystal was achieved by applying a dc bias voltage using the conductive SFM tip, as shown in Fig.1. The SBN samples for the domain engineering were prepared by the following procedure. Gold films were deposited on one side of the *c*-cut polished SBN crystals, after a poling treatment which was carried out so that the SBN crystal has a single  $180^\circ$ -domain structure (the polarization direction is parallel to the *c*-axis). The gold-coated surfaces were adhered to metal substrates using conductive paste. The crystals on the metal substrates were polished to 55–90  $\mu\text{m}$  thickness. A certain bias voltage was applied between the conductive SFM tip and the metal substrates, where the tip was grounded.

### 3. RESULTS AND DISCUSSION

#### 3.1 Domain structure of an as-grown SBN crystal

Fig.2 (a) shows the topographic image of an etched SBN. The surface was etched preferentially with a depth of approximately 5 nm. The unetched area, white in the figure, looked like islands structure with the size of a few hundred nanometers. The same region was scanned in the piezoelectric-response mode. As shown in Fig.2 (b), island-like structures appeared with dark and bright

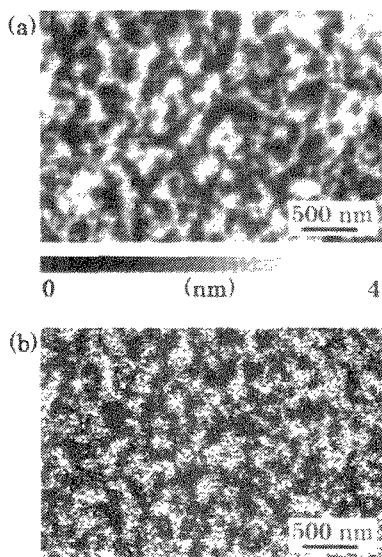


Fig.2 SFM images of the HF-etched SBN crystal (a) in the topographic mode and (b) in the piezoresponse mode. White and black areas in (a) and (b) represent the negatively and positively polarized faces of the domains, respectively.

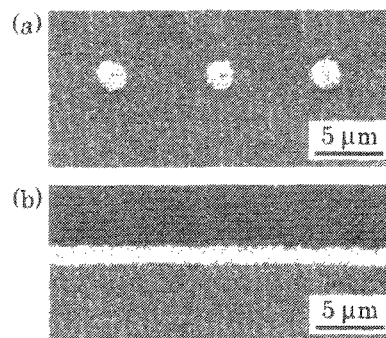


Fig.3. SFM piezoresponse images of (a) dotted inverted-domains fabricated by applying a bias voltage of  $V = -80$  V for treatment time of 40 s, and (b) linear inverted-domains fabricated by applying a bias voltage of  $V = -80$  V with scanning the cantilever at the rate of  $0.5 \mu\text{m/s}$ .

contrast. The island-like structure imaged by the piezoelectric-response mode agreed well with that of the topographic image, which suggests that the island-like structure corresponds to domain structure. It seems that the preferential etching in SBN is caused by etching rate anisotropy of  $180^\circ$  multi-domains, which was already observed in  $\text{LiNbO}_3$  [14],  $\text{LiTaO}_3$  [15] and  $\text{Pb}_{1-x}\text{Ba}_x\text{Nb}_2\text{O}_6$  [16] crystals. In order to determine the polarity of the etched regions, a SBN crystal which underwent a conventional poling treatment [17], in which negatively and positively polarized faces were formed artificially, was etched in the HF solution. The positively polarized face was determined to be preferentially etched. Thus, the white areas in Fig.2 (b) represent the negatively polarized faces of the domains.

#### 3.2 Domain engineering

We investigated the shapes of inverted domains in the SBN samples under different bias-applying condition. Fig.3 (a) shows the domains inverted by the application of voltage  $V = -80$  V for treatment time of 40 s. The inverted domains were imaged in the piezoresponse mode (represented by the white area). The polarizations of these inverted domains are directed from the surface of the crystal to the bottom; namely, the surfaces of the domains are negatively polarized. As the bias voltage increased, the inverted domains grew. In addition, when the bias voltages were fixed, the inverted domains grew as the treatment time increased. The line-shape of inverted domain was also fabricated by scanning with the conductive SFM cantilever on the SBN crystal surface while applying the voltage, as shown in Fig.3 (b). These results indicate that inverted domains with arbitrary size and shape can be fabricated using SFM by controlling the bias voltage, treatment time, and scanning condition.

We fabricated tailored-domain-patterns in the SBN crystal by scanning with the conductive SFM cantilever on the SBN crystal surface while applying a certain bias voltage. Fig.4 shows a lattice pattern of inverted domains fabricated by scanning with the conductive cantilever. In this case, the lattice pattern was fabricated by scanning with the conductive cantilever at the rate of  $1 \mu\text{m/s}$ , while applying voltage  $V = -30$  V. The width of the lines of the lattice pattern fabricated by the inverted

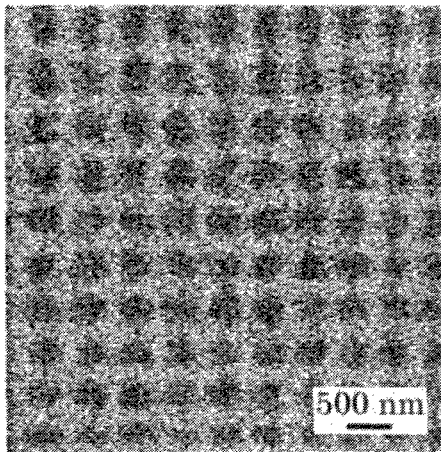


Fig.4 SFM piezoresponse image of a lattice pattern made of linear inverted-domains.

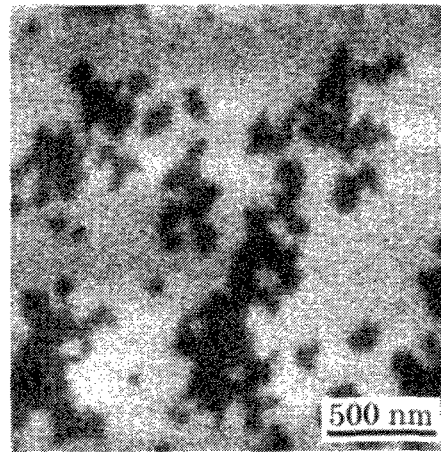


Fig.5 SFM piezoresponse image of back-switched domains in SBN crystal after the poling treatment.

domain was approximately 250 nm.

### 3.3 Back switching

In addition to the island-like domain structure naturally formed upon cooling through the Curie point to room temperature, we observed the nanoscale domain structure formed by a back switching of the inverted-domain after a conventional poling treatment. The poling treatment was carried out so that the SBN crystal has a single  $180^\circ$ -domain structure. Fig.5 shows that the piezoresponse image of nanoscale domains formed by the back switching, where the black area represents back-switched domains. The size of back-switched domains was smaller than that of island-like domains naturally formed upon cooling through the Curie point to room temperature.

### 4. CONCLUSION

We have observed the domain structure of the SBN crystal using the topographic and piezoresponse modes of the SFM. The  $180^\circ$  nanoscale island-like domains were naturally formed upon cooling through the Curie point to room temperature. Furthermore, the domain engineering was achieved by applying the appropriate bias voltage by using the SFM. We were able to pattern domain structures on microscale to nanoscale levels by controlling the magnitude of the voltage applied to the SBN samples and treatment time while scanning a conductive SFM cantilever along the sample surfaces. We consider that the fabrication technologies of nanoscale domain patterns (nanoscale domain engineering) in ferroelectric single crystals, such as a SBN crystal, by using SFM may be effective for development of novel functional devices such as photonic crystals, optical MEMS and wavelength-conversion devices.

### 5. ACKNOWLEDGEMENT

The authors would like to thank Professor Y. Cho of Tohoku University for fruitful discussions about "nanodomain engineering".

### 6. REFERENCE

- [1] K. Yamamoto, K. Mizuuchi, K. Takeshige, Y. Sasai and T. Taniuchi, *J. Appl. Phys.*, **70**, 1947 (1991).
- [2] R. W. Wallace, *Appl. Phys. Lett.*, **17**, 497 (1970).
- [3] J. A. Armstrong, N. Bloembergen, J. Duccing and P. S. Pershan, *Phys. Rev.*, **127**, 773 (1962).
- [4] K. Terabe, S. Takekawa, M. Nakamura, K. Kitamura, S. Higuchi, Y. Gotoh and A. Gruverman, *Appl. Phys. Lett.*, **81**, 2044 (2002).
- [5] K. Terabe, M. Nakamura, S. Takekawa, K. Kitamura, S. Higuchi, Y. Gotoh and Y. Cho, *Appl. Phys. Lett.*, **82** (2003) in press.
- [6] S. Kawai, T. Ogawa, H. S. Lee, R. C. DeMattei and R. S. Feigelson, *Appl. Phys. Lett.*, **73**, 768 (1998).
- [7] L. A. Bursill and P. J. Lin, *Philosophical Magazine B*, **54**, 157 (1986).
- [8] A. Gruverman, O. Auciello and H. Tokumoto, *Appl. Phys. Lett.*, **69**, 3191 (1996).
- [9] Y. G. Wang, W. Kleemann, T. Woike and R. Pankrath, *Phys. Rev. B*, **61**, 3333 (2000).
- [10] A. Gruverman, O. Auciello, J. Hatano and H. Tokumoto, *Ferroelectrics*, **184**, 11 (1996).
- [11] T. Hidaka, T. Maruyama, S. Saitoh, N. Mikoshiba, M. Shimizu, S. Shiosaki, L. A. Wills, R. Hiskes, S. A. Dicarolis and J. Amano, *Appl. Phys. Lett.*, **68**, 2358 (1996).
- [12] M. Yamada, N. Nada, M. Saitoh and K. Watanabe, *Appl. Phys. Lett.*, **62**, 435 (1993).
- [13] S. Takekawa, Y. Furukawa, M. Lee and K. Kitamura, *J. Cryst. Growth*, **229**, 238 (2001).
- [14] Y. Y. Zhu, S. N. Zhu, Z. Y. Zhang, H. Shu, J. F. Hong, G. Z. Ge and N. B. Ming, *Appl. Phys. Lett.*, **66**, 408 (1995).
- [15] K. Kitamura, Y. Furukawa, K. Niwa, V. Gopalan and T. E. Mitchell, *Appl. Phys. Lett.*, **73**, 3073 (1998).
- [16] M. Lee, R. S. Feigelson and R. K. Route, *J. Cryst. Growth*, **193**, 347 (1998).
- [17] J. E. Myers, R. C. Eckardt, M. M. Fejer, R. L. Byer, W. R. Bosenberg and J. W. Pierce, *J. Opt. Soc. Am. B*, **12**, 2102 (1995).

(Received December 21, 2002; Accepted January 31, 2003)